Bright gap solitons of atoms with repulsive interaction

B. Eiermann[1], Th. Anker[1], M. Albiez[1], M. Taglieber[1], P. Treutlein[2], K.-P. Marzlin[3], and M.K. Oberthaler[1]
[1] *Kirchhoff Institut für Physik, Universität Heidelberg, Im Neuenheimer Feld 227, 69120 Heidelberg, Germany*
[2] *Max-Planck-Institut für Quantenoptik und Sektion Physik der Ludwig-Maximilians-Universität, Schellingstr.4, 80799 München, Germany*
[3] *Quantum Information Science Group Department of Physics and Astronomy 2500 University Drive NW Calgary, Alberta T2N 1N4 Canada*
(Dated: December 13, 2013)

We report on the first experimental observation of bright matter-wave solitons for ^{8}7Rb atoms with repulsive atom-atom interaction. This counter intuitive situation arises inside a weak periodic potential, where anomalous dispersion can be realized at the Brillouin zone boundary. If the coherent atomic wavepacket is prepared at the corresponding band edge a bright soliton is formed inside the gap. The strength of our system is the precise control of preparation and real time manipulation, allowing the systematic investigation of gap solitons.

PACS numbers: 03.75.Be, 03.75.Lm, 05.45.Yv, 05.45.a
Keywords:

Non-spreading localized wave packets [1] - bright solitons - are a paradigm of nonlinear wave dynamics and are encountered in many different fields, such as physics, biology, oceanography, and telecommunication. Solitons form if nonlinear dynamics compensates the spreading due to linear dispersion.

For atomic matter waves, bright solitons have been demonstrated where the linear spreading due to vacuum dispersion is compensated by the attractive interaction between atoms [2]. For repulsive atom-atom interaction dark solitons have also been observed experimentally [3].

In this letter we report on the experimental observation of a different class of solitons, which only exist in periodic potentials - bright gap solitons. For weak periodic potentials formation of atomic gap solitons has been predicted [4] while discrete solitons [5] should be observable in the case of deep periodic potentials. These phenomena are well known in the field of nonlinear photon optics where the nonlinear propagation properties in periodic refractive index structures have been studied [6]. In our experiments with interacting atoms a new level of experimental control can be achieved allowing for the realization of standing gap solitons for repulsive atom-atom interaction corresponding to a self-defocussing medium. It also opens up the way to study driven solitons [7] and the realization of two- and three dimensional discrete solitons [8].

In our experiment we investigate the evolution of a Bose-Einstein condensate in a quasi one-dimensional waveguide with a weak periodic potential superimposed in the direction of the waveguide. In the limit of weak atom-atom interaction the presence of the periodic potential leads to a modification of the linear propagation i.e. dispersion [9]. It has been demonstrated that anomalous dispersion can be realized with this system [10] which is the prerequisite for the realization of bright gap solitons for repulsive atom-atom interaction.

Our experimental observations are shown in figure 1 and clearly reveal that after a propagation time of 25ms a non-spreading wave packet is formed. The observed behavior exhibits the qualitative features of bright gap soliton formation such as: (a) during soliton formation excessive atoms are radiated and spread out over time (b) solitons do not change their shape and atom number during propagation (c) gap solitons do not move.

The coherent matter-wave packets are generated with ^{87}Rb Bose-Einstein condensates (figure 2a). The atoms

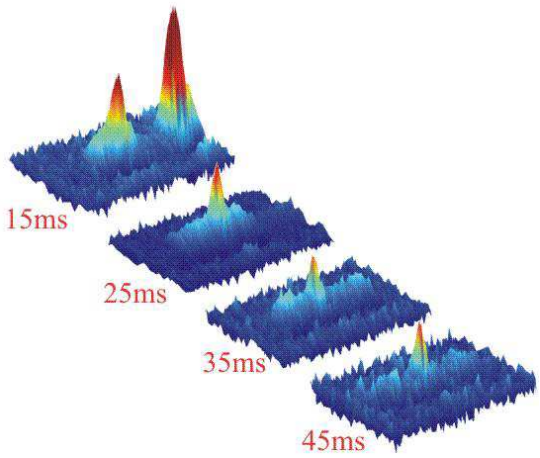

FIG. 1: Observation of bright atomic gap solitons. The atomic density in the negative mass regime deduced from absorption images (430μm x 125μm) averaged over 4 realizations is shown for different propagation times. After approximately 25ms a small peak is formed which does neither change in shape nor in amplitude. Excessive atoms are radiated and disperse over time. After 45ms only the soliton with $\sim$250 atoms has sufficient density to be clearly observable. The second peak at 15ms shows the atoms which have been removed by Bragg scattering to generate an initial coherent wave packet consisting of $\sim$900 atoms.

are initially precooled in a magnetic TOP trap using the standard technique of forced evaporation leading to a phase space density of ∼0.03. The atomic ensemble is subsequently adiabatically transferred into a crossed light beam dipole trap (λ=1064nm, $1/e^2$ waist 60 μm, 500mW per beam) where further forced evaporation is achieved by lowering the light intensity in the trapping light beams. With this approach we can generate pure condensates with typically 3×10^4 atoms. By further lowering the light intensity we can reliably produce coherent wave packets of 3000 atoms. For the successful demonstration of gap solitons further reduction of the atom number is necessary. For that purpose we employ a Bragg pulse in the trap allowing the preparation of coherent wave packets of $\sim$ 900 atoms.

After the preparation of the coherent wave packet a periodic dipole potential realized with a far off-resonant standing light wave of wavelength $\lambda = 783$nm (figure 2b), is adiabatically ramped up. As indicated in figure 2 this procedure prepares the atomic ensemble in the normal dispersion regime at quasimomentum $q = 0$. The dispersion relation for an atom moving in a weak periodic potential exhibits a band structure as a function of quasimomentum q known from the dispersion relation of electrons in crystals [11] (see figure 2e). Anomalous dispersion, characterized by a negative effective mass $m_{\rm eff} < 0$, can be achieved if the mean quasimomentum of the atomic ensemble is shifted to the Brillouin zone boundary corresponding to $q = \pi/d$. This is accomplished by switching off one dipole trap beam, releasing the atomic cloud into the one-dimensional horizontal waveguide (Fig. 2c) with transverse and longitudinal trapping frequencies $\omega_\perp = 2\pi \times 85$Hz and $w_{||} = 2\pi \times 0.5$Hz. Subsequently the atomic ensemble is prepared at quasimomentum $q = \pi/d$ by accelerating the periodic potential to the recoil velocity $v_r = h/m\lambda$. The acceleration within 1.3ms is adiabatic, therefore excitations to the upper bands are negligible [12]. It is important to note that the strength of dispersion and correspondingly the absolute value of $m_{\rm eff}$ is under full experimental control, since it scales with the modulation depth of the periodic potential.

For weak periodic potentials the full wavefunction of the condensate is well described by $\Psi(x,t) = A(x,t)u_0^{q_c}(x)\exp(iq_cx)$, where $u_0^{q_c}(x)\exp(iq_cx)$ represents the Bloch state in the lowest band $n = 0$ at the corresponding central quasimomentum q_c. Within the approximation of constant effective mass, the dynamics of the envelope $A(x,t)$ is governed, by a one-dimensional nonlinear Schrödinger equation [13]

$$i\hbar\frac{\partial}{\partial t}A(x,t) = \left(-\frac{\hbar^2}{2m_{\rm eff}}\frac{\partial^2}{\partial x^2} + g_{1d}|A(x,t)|^2\right)A(x,t)$$

with $g_{1d} = 2\hbar a\omega_\perp\alpha_{nl}$ where α_{nl} is a renormalization factor due to the presence of the periodic potential (α_{nl} =1.5 for $q = \pi/d$ in the limit of weak periodic potentials [13]),

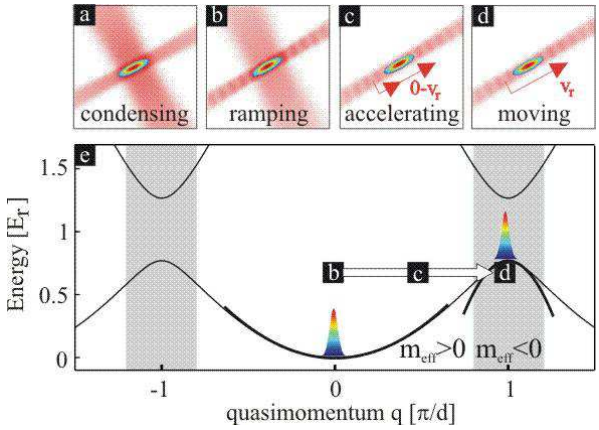

FIG. 2: Realization of coherent atomic wavepackets with negative effective mass utilizing periodic potentials. (a) top view of the crossed dipole trap geometry used for Bose-Einstein condensation. (b) a periodic potential is ramped up while the atoms are still trapped in the crossed dipole trap realizing the atomic ensemble at $q_c = 0$. (c,d) the atoms are released into the one-dimensional waveguide and subsequently the periodic potential is accelerated to the recoil velocity $v_r = h/\lambda m$. This prepares the atomic wavepacket at the band edge of the lowest band. (e) normal and anomalous dispersion regime in a periodic potential. The single preparation steps are indicated. The shown band structure is calculated for the experimentally employed potential modulation depth of V=0.7 E_r leading to $m_{\rm eff}/m = -0.1$ at the band edge.

and a is the scattering length. The stationary solution for $q_c = \pi/d$ is given by

$$A(x,t) = \sqrt{N/2x_0}\,\mathrm{sech}(x/x_0)e^{i\hbar t/2m_{\rm eff}x_0^2},$$

where x_0 is the soliton width and $m_{\rm eff}$ is the effective mass at the band edge.

The quantitative features of bright solitons can be understood through comparison of the characteristic energies for dispersion and atom-atom interaction. The linear spreading is characterized by the energy $E_D = \hbar^2/2m_{\rm eff}x_0^2$. The atom-atom interaction is given by $E_{nl} = g_{1d}|A(x=0,t)|^2$. Equating both energies, leads to the total number of atoms constituting the soliton

$$N = \frac{\hbar}{\alpha_{nl}a\omega_\perp m_{\rm eff}x_0}. \qquad (1)$$

A characteristic time scale of solitonic propagation due to the phase evolution can also be identified. In analogy to light optics the soliton period is given by $T_S = \pi m_{\rm eff}x_0^2/2\hbar$. Solitonic propagation can be confirmed experimentally if the wave packet does not broaden over time periods much longer than T_S.

Our experimental results in figure 1 show the evolution of a matter wave soliton in the negative mass regime for different propagation times. The reproducible formation of a single soliton is observed if the initial wave packet is close to the soliton condition, i.e. a well defined

atom number for a given spatial width. Our experimental setup allows the reliable production of condensates which contain not less than 3000 atoms with a spatial size of $\sim 2.5\mu$m (rms) resulting from the longitudinal trapping frequency of the crossed dipole trap $\sim 40 \times 2\pi$Hz. For this atom number no gap solitons have been observed. Therefore we remove 70% of the atoms by Bragg scattering leading to an inital wavepacket with 900(300) atoms. As shown in figure 1, the Bragg scattered atoms are still visible after 15ms and move out of the imaged region for longer observation times. The soliton can clearly be distinguished from the background after 25ms, corresponding to 3 soliton periods. This is consistent with the typical formation time scale of few soliton periods given in nonlinear optics text books [14]. After 45ms of propagation, the density of the radiated atoms drops below the level of detection and thus a pure soliton remains, which has been observed for up to 65ms. In order to understand the background we numerically integrated the nonpolynomial nonlinear Schrödinger equation [15]. The calculation reveals that the non-quadratic dispersion relation in a periodic potential leads to an initial radiation of atoms. However the absolute number of atoms in the observed background is much higher than the prediction of the employed effective one-dimensional model. Therefore we conclude that transverse excitations have to be taken into account to get quantitative agreement. This fact still has to be investigated in more detail.

In the following we will discuss the experimental facts shown in figure 3 and figure 4 confirming the successful realization of atomic bright gap solitons.

In figure 3a we compare the spreading of wave packets in the normal and anomalous regime which reveals the expected dramatic difference in wave packet dynamics. The solid circles represent the width of the gap soliton for $m_{\rm eff}/m = -0.1$, which does not change significantly over time. In this regime, the wave packet does not spread for more than 8 soliton periods ($T_S = 7.7$ms). We deduce a soliton width of $x_0 = 6(1)\mu m$ ($x_{rms} = 4.5\mu$m) from the absorption images where the measured rms width shown in figure 3a is deconvolved with the optical resolution of 3.8μm (rms). Since our experimental setup allows to switch from solitonic to dispersive behavior by turning the periodic potential on and off, we can directly compare the solitonic evolution to the expected spreading in the normal dispersion regime. The open circles represent the expansion of a coherent matter wave packet with 300(100) atoms in the normal mass regime $m_{\rm eff}/m = 1$.

The preparation at the band edge implies that the group velocity of the soliton vanishes. This is confirmed in figure 3b, where the relative position of the soliton with respect to the standing light wave is shown. The maximum group velocity of the lowest band is indicated with the dotted lines. In the experiment care has to be taken to align the optical dipole trap perpendicular to the gravitational acceleration within 200μrads. Otherwise the solitons are accelerated in the direction opposite to the gravitational force revealing their negative mass characteristic.

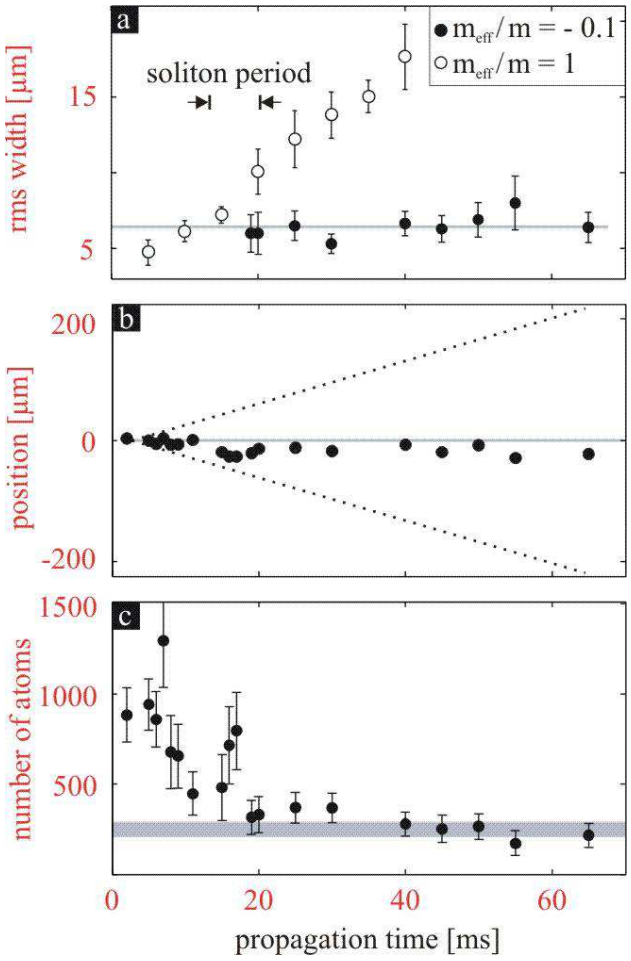

FIG. 3: Characteristic features of the observed gap soliton. (a) Comparison of expansion in the positive and negative effective mass regime for 300 atoms. While the soliton does not disperse at all over a time of 65ms, corresponding to more than 8 soliton periods (solid circles), a wave packet in the normal mass regime expands significantly (open circles). Each point represents the result of a single realization. (b) shows the position of the soliton in the frame of the periodic potential and reveals that a standing gap soliton has been realized. The dotted lines indicate the positions that correspond to maximum and minimum group velocity in the lowest band. (c) number of atoms in the central peak. The initial atom numbers exhibit large shot to shot fluctuations, which are reduced during the soliton formation. The predicted relation between the number of atoms and the soliton width (eq. 1) is indicated by the horizontal bar in graph c using the width deduced as shown in graph (a). Note that this comparison has been done without free parameter and all contributing parameters are measured independently.

The calculated number of atoms (eq.1) is indicated by the horizontal bar in figure 3c. The width of the bar represents the expectation within our measurement un-

certainties. The observed relation between atom number and width, characteristic for a bright soliton, is in excellent agreement with the simple theoretical prediction without any free parameter.

As an additional check for soliton formation, we determine the product of atom number and soliton width as a function of the effective mass which is varied by adjusting the modulation depth of the periodic potential. Figure 4 shows the range of effective masses, for which solitons have been observed. For smaller values of $|m_{\rm eff}|$, corresponding to smaller potential depths, Landau-Zener Tunneling does not allow a clean preparation in the negative mass regime, while for larger values the initial number of atoms differs too much from the soliton condition. The observed product of atom number and wave packet width after 40ms of propagation are shown in figure 4 and confirm the behaviour expected from eq.1. Additionally, our experimental findings reveal that the change of the scaling parameter Nx_0 in figure 4 is dominated by the change in the atom number, while the soliton width only exhibits a weak dependence on the effective mass.

The demonstration of standing atomic gap solitons confirms that Bose condensed atoms combined with a periodic potential allow the precise control of dispersion and nonlinearity. Thus our setup serves as a versatile new model system for nonlinear wave dynamics. Our experiments show that atomic gap solitons can be created in a reproducible manner. This is an essential prerequisite for the study of soliton collisions. The experiment can be realized by preparing two spatially separated wavepackets at the band edge and applying an expulsive potential. Ultimately, atom number squeezed states can be engineered with atomic solitons by implementing schemes analog to those developed for photon number squeezing in light optics [16]. This is interesting from a fundamental point of view and may also have impact on precision atom interferometry experiments.

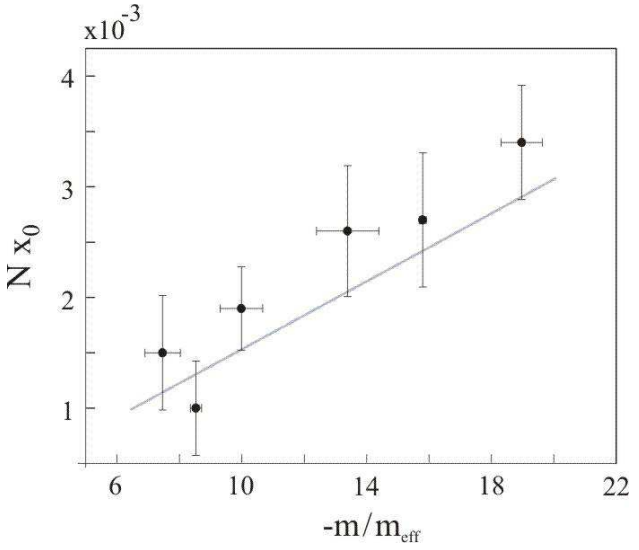

FIG. 4: Scaling properties of an atomic gap soliton. The effective mass was varied experimentally by changing the periodic potential depth. The scaling predicted by (eq.1) is represented by the solid line and is in excellent agreement with our experimental observations. The errorbars represent the variation of the scaling parameter for different realizations.

We wish to thank J. Mlynek for his generous support, Y. Kivshar, E. Ostrovskaya, A. Sizmann and B. Brezger for many stimulating discussions. We thank O. Vogelsang and D. Weise for their donation of Ti:Sapphire light. This work was supported by Deutsche Forschungsgemeinschaft, Emmy Noether Program, and by the European Union, Contract No. HPRN-CT-2000-00125.

[1] J.S. Russel , Report of the 14th meeting of the British Association for the Advancement of Science, 311-390, Plates XLVII-LVII (1845).

[2] L. Khaykovich, et al., Science **296**, 1290-93 (2002). K.E. Strecker, G.B. Partridge, A.G. Truscott and R.G. Hulet, Nature **417**, 150-153 (2002).

[3] S. Burger, K. Bongs, S. Dettmer, W. Ertmer, K. Sengstock, Phys. Rev. Lett. **83**, 5198-5201 (1999). J. Denschlag et al., Science **287**, 97-100 (2000).

[4] P. Meystre, *Atom Optics* (Springer Verlag, New York, 2001) p 205, and references therein.

[5] A. Trombettoni and A. Smerzi, Phys. Rev. Lett. **86**, 2353 (2001).

[6] R.J. Eggleton, R.E. Slusher, C.M. deSterke, P.A. Krug, and J.E. Sipe, Phys. Rev. Lett. **76**, 1627 (1996). C.M. de Sterke, and J.E. Sipe, Progress in Optics, **33** 203 (1994). D. Neshev, A.A. Sukhorukov, B. Hanna, W. Krolikowski, and Y. Kivshar cond-mat 0311059 (2003).

[7] H. Saito, and M. Ueda, Phys.Rev.Lett. **90**, 040403 (2003).

[8] E. A. Ostrovskaya and Yu. S. Kivshar, Phys. Rev. Lett. **90**, 160407 (2003), V. Ahufinger, A. Sanpera, P. Pedri, L. Santos, M. Lewenstein cond-mat 0310042 (2003).

[9] S. Burger, F.S. Cataliotti, C. Fort, F. Minardi, M. Inguscio, M.L. Chiofalo, and M.P. Tosi, Phys. Rev. Lett. **86**, 4447 (2001).

[10] B. Eiermann, P. Treutlein, Th. Anker, M. Albiez, M. Taglieber, K.-P. Marzlin, and M.K. Oberthaler, Phys.Rev.Lett. **91**, 060402 (2003).

[11] N. Ashcroft and N. Mermin, *Solid State Physics* (Saunders, Philadelphia, 1976).

[12] B.P. Anderson, and M.A. Kasevich, Science **282** 1686 (1998); O. Morsch, J. Müller, M. Cristiani, D. Ciampini, and E. Arimondo, Phys. Rev. Lett. **87**, 140402 (2001).

[13] M. Steel and W. Zhang, cond-mat/9810284 (1998).

[14] G.P. Agrawal, *Applications of Nonlinear Fiber Optics* (Academic Press, San Diego, 2001). G.P. Agrawal, *Nonlinear Fiber Optics* (Academic Press, San Diego, 1995).

[15] L. Salasnich, A. Parola, and L. Reatto, Phys.Rev. A **65**, 043614 (2002).

[16] S.R. Friberg, S. Machida, M.J. Werner, A. Levanon, and T. Mukai, Phys. Rev. Lett. **77**, 3775 (1996).